

INFLUENCE OF CONTROL CURRENT WAVEFORM ON ROTOR NUTATION OF THREE-DEGREES-OF-FREEDOM ELECTRIC MACHINE

I.S. Petukhov*, K.P. Akinin**, V.G. Kireyev***, V.A. Lavrinenko

Institute of Electrodynamics National Academy of Sciences of Ukraine,
Beresteiskyi Ave., 56, Kyiv, 03057, Ukraine.

E-mail: igor_petu@ukr.net.

The design of the electric machine with three degrees of freedom of the rotor with an external magnetic core, containing permanent magnets, and an internal magnetic core is considered. The both magnetic cores are rotating. The stator windings (control winding and two-phase rotation winding) are located in the air gap between the magnetic cores. The windings are powered by alternating current of corresponding phase. The positive property of rotor gyro-stabilization in such structure is shown. At the same time, the negative fact consists in the nutation under the conditions of forced change in the orientation of rotation axis. There are no magnetic losses in the structure due to synchronous rotation of both external and internal magnetic cores. The immobility of the center of mass is assumed. There are no losses that give a non-conservative mechanical system. The mathematical model of the mechanic system and magnetic field is developed to compute the electromagnetic torques acting on the rotor. The expressions for electromagnetic torque components are obtained to use them in the Comsol Multiphysics interface. The effect of the sinusoidal and pulse currents in the control winding on the nutation swing is studied. The optimality of the control winding supplied by undisturbed sinusoidal current or the pulse current having square-wave length of about one-third of the period is revealed. References 15, figures 6, table 1.

Keywords: three-degree-of-freedom electric machine, gyro-stabilization, electromagnetic torque, control winding, precession, nutation.

Introduction. The electric machines/drives with three degrees of freedom (3-DOF) are used in the tracking and observation systems and are often located on moving and fixed objects. In such applications, there are strict requirements for image stabilization of an observation object. The stabilization problem is realized in different ways. Some of them are to use both the four-pole [1, 2, 3] and complex multi-pole magnetic system based on the stepping motor principle [4, 5, 6]. The structure with a liquid suspension of the rotor is known [7]. The other way is to use the switching reluctance principle [8]. All of the above-mentioned actuators have a complicated magnetic system and control unit which is complicated too.

The principle of gyro-stabilization is used in different cases. Then the movable structural element, in fact, the rotor, is rotated at high speed [9, 10]. Such machines have a spherical configuration of the active volume and include the internal compact gimbal suspension. They can be constructed with a simple two-pole magnetic system. The high-speed rotation of the rotor causes the nutation phenomenon, which is inherent largely to axial symmetric rotating objects. The nutation occurs when the rotor is affected by external forces and performs precession movement [11]. As a result, in these observation systems, the image sharpness of observed object is decreasing. The different damping devices are used to level the nutation. Additionally, the time dependence of rotor control torques has an influence on the nutation amplitude. Thus, for the tracking system [9], the control winding powered by sinusoidal current is used to control the gyro-stabilized 3-DOF rotor. This structure has the better energy, speed, mass and dimensional performances in comparison with the classic gyroscopic constructions with separate drives for each coordinate [9, 10]. However the sinusoidal current needs a more complicated inverter for power supply than the inverter with a square voltage pulse. The inverter and its control circuit are the important components that determine the complexity of the electromechanical system.

Accordingly the *aim of the article* is to study the effect of control current waveform on the nutation range of rotor.

Structure of machine active volume. The exterior rotor 3-DOF machine, having the outer rotor with permanent magnets and internal magnetic yoke that are both rotating synchronously, is studied. Some positive features of the structure are noted in [9]. In particular, as for such a structure there are no eddy currents and hysteresis losses due to the both yokes are rotated. In addition, the external rotor has a significant

© Petukhov I.S., Akinin K.P., Kireyev V.G., Lavrinenko V.A., 2023

ORCID ID: * <https://orcid.org/0000-0003-1416-1174>; ** <https://orcid.org/0000-0002-7830-2311>;

*** <https://orcid.org/0000-0002-9407-1074>

moment of inertia that positively influences on nutation swing and drift of the rotation axis caused by the losses of any nature. The half of the magnetic system of the machine and its cross-section are shown in Fig. 1. The system of windings consisting of two lumped rotational windings and control winding [9] is considered. It is necessary to note that the internal magnetic yoke shunts the magnetic field which can penetrate into the metallic gimbal suspension located in the center of rotation and causes the losses.

The structure of the machine is not symmetric relative to the plane normal to the axis of rotation. For the manufacture aim the windings shifted along the Z-axis and the values of angles α_1 and α_2 differ from each other (Fig. 1). The symmetric structure is chosen for study because it offers high performance and might be as a benchmark to compare with a real unit.

When the control winding is supplied by sinusoidal current with the frequency equal to the rotation speed, the pulsed electromagnetic moment arises and provides the tilt of the rotor in any of two mutually perpendicular angle coordinates [9]. The direction of the tilt is defined by current phase. The rotational windings are placed under control winding (Fig. 1) and shifted by 90° between each other.

Mathematical model. As mentioned above, the nutation is caused by the changing direction of the rotation axis due to precession. To focus on the studied phenomenon, all secondary factors that can depend on the specific design of the device or the conditions of its operation are neglected. For the above reason, the second idealization in the study consists in disregard for the influence of the windings of rotational motion. These windings produce the additional deflection torque when the angle of nutation differs from zero. Thus the process of free rotation is studied.

Another idealization is to neglect any forces that give a non-conservative system. These forces may result from friction in bearings, aerodynamic and magnetic losses and damping devices. As mentioned above, the elimination of the magnetic losses is realized owing to all rotating magnetic cores.

Finally, the motion of the rotor in an inertial coordinate system is considered. The following assumptions are made to formulate the mathematical model.

1. The center of mass of the 3-DOF rotor is stationary.
2. There is no influence of rotation windings.
3. Only electromagnetic control torques act on the rotor, and any other torques are not taken into account.

4. The entire rotor structure is assumed to be a rigid body (no damping units).

In the case of rotational motion of the body relative to a fixed point, the axes of the coordinate system lying in the planes of symmetry are the basic axes of inertia. Then Euler dynamic equations have the form [12]:

$$\begin{cases} I_{xx} \dot{\omega}_x - (I_{yy} - I_{zz}) \omega_y \omega_z = M_x; \\ I_{yy} \dot{\omega}_y - (I_{zz} - I_{xx}) \omega_z \omega_x = M_y; \\ I_{zz} \dot{\omega}_z - (I_{xx} - I_{yy}) \omega_x \omega_y = M_z; \end{cases} \quad (1)$$

where I_{xx} , I_{yy} and I_{zz} are the moments of inertia relative to corresponding axes; ω_x , ω_y , ω_z are the angular velocities relatively mentioned axes, the point above the variables means the total derivative with respect to time; M_x , M_y and M_z are the external torques.

The solution of equations (1) is implemented in the Multibody Dynamics interface of Comsol Multiphysics [13]. This interface takes into account all the features of gyroscopic effect; the input data describes the geometry of the body, the properties of materials and the electromagnetic torques that are present on the

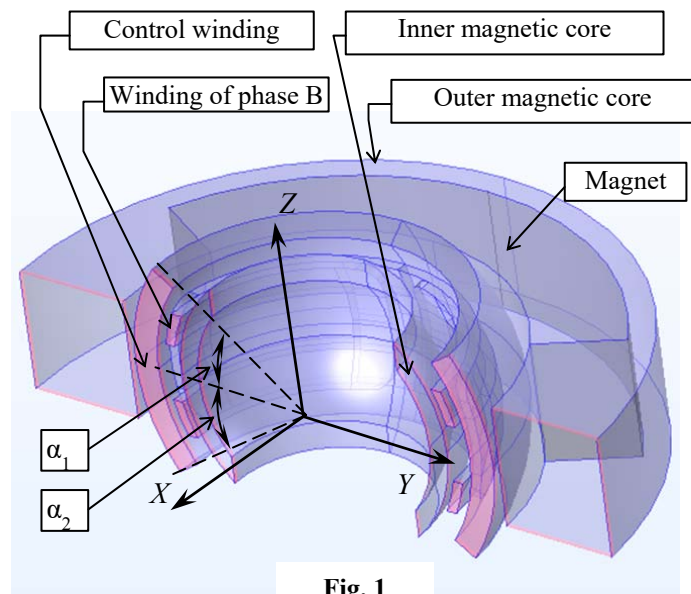


Fig. 1

right-hand side of equations (1). Due to neglecting the eddy currents and magnetic hysteresis, the magnetic field is assumed to be magnetostatic. Then the electromagnetic torques as well as their dependence on orientation angles can be computed previously in the Magnetic Fields interface of Comsol Multiphysics [13], but not calculated in the integration process of movement equations (1).

The magnetostatic field of magnetic system with nonlinear ferromagnetic materials and residual magnetization is described by the system of equations for the vector magnetic potential variable \mathbf{A} in three-dimensional model:

$$\begin{cases} \nabla \times \left(f(\|\mathbf{B}\|) \frac{\mathbf{B}}{\|\mathbf{B}\|} - H_c \frac{\mathbf{e}}{\|\mathbf{e}\|} \right) = \mathbf{J}_{wc}; \\ \mathbf{B} = \nabla \times \mathbf{A}; \end{cases} \quad (2)$$

where ∇ is the Hamilton's operator; $f(\|\mathbf{B}\|)$ is the dependence of magnetic field on magnetic flux density; \mathbf{B} is the magnetic flux density vector; H_c is the coercive force of the magnet; \mathbf{e} is the unit vector; \mathbf{J}_{wc} is the external current density in control winding domain. The coercive force is zero within the domains of the soft iron and air. To take into account magnetic field propagation outside the external magnetic core, the magnetic domains in the Comsol model are surrounded by an air domain within the 4-time external radius R_a of the core. The layer with $0,5R_a$ thickness is placed under the external surface of this sphere and filled with infinite elements [13].

The computation of the electromagnetic moment components included in equations (1) in Magnetic Fields interface is performed by integration of the components of corresponding electromagnetic forces. For this slotless structure of the 3-DOF electric machine the Lorentz formula [13] is used to calculate the components of electromagnetic force

$$\mathbf{F} = \mathbf{J} \times \mathbf{B}, \quad (3)$$

where \mathbf{J} is the current density vector. In turn, the components of electromagnetic torque M_x, M_y in the stator frame (x, y, z) can be determined by integration of the spatial components of electromagnetic force over the domain V_C of the control winding according to the expressions:

$$\begin{cases} M_x = \int_{V_C} (F_x \cdot z - F_z \cdot x) dV, \\ M_y = \int_{V_C} (-F_y \cdot z + F_z \cdot y) dV \end{cases}, \quad (4)$$

where F_x, F_y and F_z are the corresponding components of Lorentz force (3).

Electromagnetic torques for precession control. In the theory of electrical machines, the representation of the magnetic field in the air gap by harmonic series is traditional. In this case, each harmonic of any variable including magnetic flux density, magnetic flux linkage, MMF can be considered as a spatial vector. As shown in [9] the field distribution in the air gap of the structure under consideration is quite close to sinusoidal. Then we can restrict ourselves to only first (fundamental) harmonic for vector representation of the flux linkage and MMF of control winding. Note that the MMF vector of control winding is the current multiplied by the number of turns of this winding.

As the nutation is the vibration of rotation axis during the process of forced precession, the Rezal [12] (Tait-Bryan [14]) angles in order $(y-x-z)$ are acceptable to illustrate the nutation process. The sequence of rotation from stator coordinate system (x, y, z) to rotor coordinate system (D, Q, Z) in the proposed order is shown in Fig. 2.

The expression for electromagnetic torque due to the interaction of the control winding current i_c and the flux linkage vector of the magnetized rotor $\Psi_D = (\Psi_x, \Psi_y, \Psi_z)$ in stator coordinates (x, y, z) is the vector product:

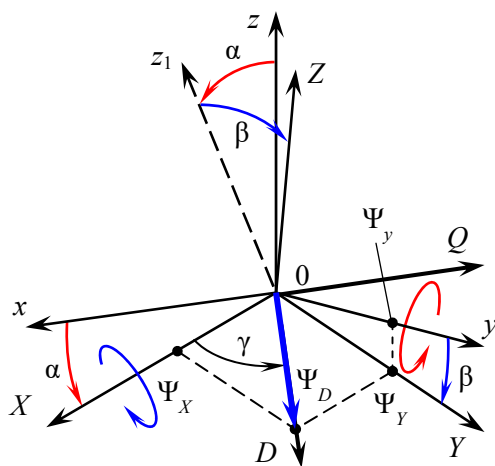


Fig. 2

$$\mathbf{M} = -\det \begin{bmatrix} \vec{i} & \vec{j} & \vec{k} \\ \Psi_x & \Psi_y & \Psi_z \\ 0 & 0 & i_C \end{bmatrix}, \quad (5)$$

where $\vec{i}, \vec{j}, \vec{k}$ are the unit vectors of the Cartesian coordinate system of stator.

Then the expressions for torque components in the stator frame are as follows:

$$\begin{bmatrix} M_x \\ M_y \end{bmatrix} = \begin{bmatrix} -\Psi_y \\ \Psi_x \end{bmatrix} i_C. \quad (6)$$

The magnetic-flux linkage components of the excitation system in the initial frame of the rotor (X, Y, Z) are the sinusoidal functions of rotating angle γ :

$$\begin{bmatrix} \Psi_X \\ \Psi_Y \end{bmatrix} = \Psi_D \begin{bmatrix} \cos \gamma \\ \sin \gamma \end{bmatrix}. \quad (7)$$

The multiplication of expression (7) on the left of inverse rotation matrix sequentially by angle $(-\beta)$ and angle $(-\alpha)$:

$$\begin{bmatrix} \Psi_x \\ \Psi_y \\ \Psi_z \end{bmatrix} = \begin{bmatrix} \cos \alpha & 0 & -\sin \alpha \\ 0 & 1 & 0 \\ -\sin \alpha & 0 & \cos \alpha \end{bmatrix} \begin{bmatrix} 1 & 0 \\ 0 & \cos \beta \\ 0 & -\sin \beta \end{bmatrix} \begin{bmatrix} \Psi_X \\ \Psi_Y \end{bmatrix} \quad (8)$$

gives the expressions for magnetic-flux linkage components in the stator frame according to expressions (7) and (8):

$$\begin{bmatrix} \Psi_x \\ \Psi_y \\ \Psi_z \end{bmatrix} = \begin{bmatrix} \cos \alpha \cos \gamma + \sin \alpha \sin \beta \sin \gamma \\ \cos \beta \sin \gamma \\ -\sin \alpha \cos \gamma - \cos \alpha \sin \beta \sin \gamma \end{bmatrix} \Psi_D. \quad (9)$$

The component Ψ_y can be shown in Fig. 2 as it has a simple expression (see (9)). According to (6), the expressions for electromagnetic torque are:

$$\begin{cases} M_x = -(\cos \beta \sin \gamma) \Psi_D i_C \\ M_y = (\cos \alpha \cos \gamma + \sin \alpha \sin \beta \sin \gamma) \Psi_D i_C \end{cases}. \quad (10)$$

The resulting expressions (10) give the complete dependences of electromagnetic moment components on the inclination angles and rotation angle of the rotor. These expressions contain the instantaneous value of the control current i_C and the harmonic dependence of the magnetic flux linkage of the control winding on the Rezal angles. The harmonic expressions are quite acceptable for approximation relative to this task [9, 15]. The results of three-dimensional field simulation are used to find the amplitude Ψ_D for minimization of approximation error in expression (10). That is, the mentioned amplitude Ψ_D is estimated through the moments determined by integral relations (4) under the condition of the maximum value of these moments and fixed current i_C [15]. The expressions (10) form the input data for the moment (in fact, torque) components in the Multibody Dynamics interface of Comsol Multiphysics to simulate the equations (1).

Results and discussion. The results of preliminary tests show that the typical form of locus (Fig. 3) of the rotational axis location at angle coordinates (α, β) is characterized by the beat oscillations with the same in value amplitudes along both coordinates. Therefore the only time dependence of the oscillation angle β (or α) can be considered to define the nutation characteristic. The sample in Fig. 3 corresponds to the case when the external torque acts about axis x . Consequently, the precession takes place around axis y .

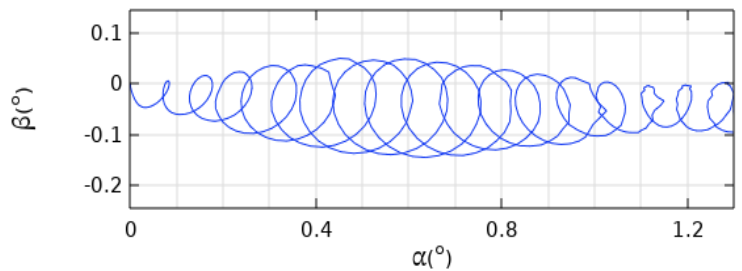


Fig. 3

Initially, the study is focused on analyzing the disturbance caused by the sinusoidal waveform of control current. The disturbance is realized by **sin** function according to the formula:

$$i_c(t) = kI_{eff}I_C \sin^m(\Omega t + \psi), \quad (11)$$

where t is the time; kI_{eff} is the scaling coefficient; I_C is the control current amplitude; Ω is the angular frequency of the current; ψ is the initial phase.

It is important to note that the angular frequency Ω is equal to the rotation angular frequency of the

Parameter	Value
Total air gap between magnetic cores (4.5 mm)	0.104*
Thickness of windings layer (3.5 mm)	0.081*
Height of the yoke of internal core (1.5 mm)	0.035*
Height of the yoke of external core (2 mm)	0.045*
Length of magnet along magnetization axis (7 mm)	0.162*
Angular size of magnet (X, Y plane, Fig. 1)	120°
Angular size of control winding (X, Z plane)	70°
Angular span of rotation winding (X, Y plane)	154°
Angular width of the active part of rotation winding section	13°
Ratio of control winding thickness to rotation winding thickness	8/3
Space factor of copper windings	0,34
Material of permanent magnet	KC37A
Current density of control winding, A/mm ²	10
Angular frequency of rotational rotor speed, rpm	6000
Resistance of control winding (per turn), Ohm	0.0021
Inductance of control winding (per turn), H	6.2·10 ⁻⁸

rotor because the structure of the 3-DOF machine under consideration has always two poles. The geometric and regime data of the model are presented in Table (the asterisks indicate the dimensions relative to the pole pitch).

The plots in Fig. 4 show the dependence of the fluctuations of β angle on time with different values of exponent m in expression (11). The constant torque that has the corresponding amplitude is studied along with to the torque caused by alternating current. It is should be noted that this moment cannot be achieved with any current waveform and is used only for theoretical investigation.

All considered processes have the start point $(\alpha, \beta) = (0, 0)$, but the plots are shifted at different distances along the y -axis for visualization. The coefficient kI_{eff} is taken into account in expression (11) to provide the constant RMS of control current in all variants. The forced precession angle α is set to be 0 by assigning the initial zero current phase ψ in (11). The computational results show that the minimal nutation swing is observed in the case of constant torque of about 0.025°. The torque produced by sinusoidal current

has two times greater swing (about 0.05°). Any disturbance of sinusoidal form leads to a substantial increase in nutation swing.

The power supply of control winding by inverter with square output voltage is described below. Fig. 5 shows the control winding currents for different values of square pulse angular length D of output inverter voltage.

The current is calculated taking into account the time constant τ_C of the control winding circuit:

$$\tau_C = L_C / r_C, \quad (12)$$

where L_C and r_C are the inductance and resistance of the circuit, respectively (see Table).

Note that the inductance of the winding is computed in the Magnetic Fields interface ignoring magnetization of the magnets.

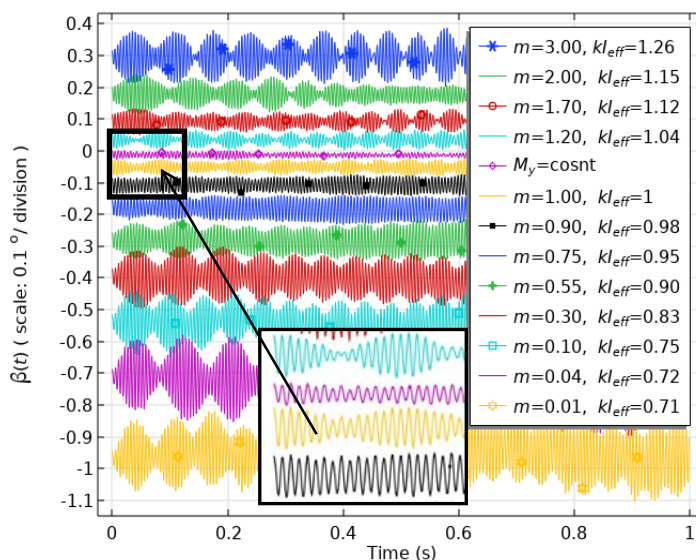


Fig. 4

Time dependencies of the angle β corresponding to pulse waveforms in Fig. 5 are presented in Fig. 6 (the graphs are shifted as mentioned above). In this case, the minimum nutation swing corresponds to the pulse angular length of 120 electrical degrees. The value of the swing is equal to approximately 0.05° at ideal sinusoidal current (Fig. 4). But in the case of pulse power supply, there is the deviation of average trajectory of rotation axis from x -axis; it can be seen in Fig. 6 already at time of 0.05 s. The reason for this deviation consists in the asymmetric current pulse caused by transient processes at their rise and drop (Fig. 5). The minimal nutation swing may be due to a particular current spectrum. The uniqueness of the pulse angular length equal to 120 electrical degrees consists in the lack of the third harmonic in the spectrum. Rather, the third harmonic content in this pulse waveform (Fig. 5) is more 20 times less than in the pulses with length of 90 and 150 electrical degrees.

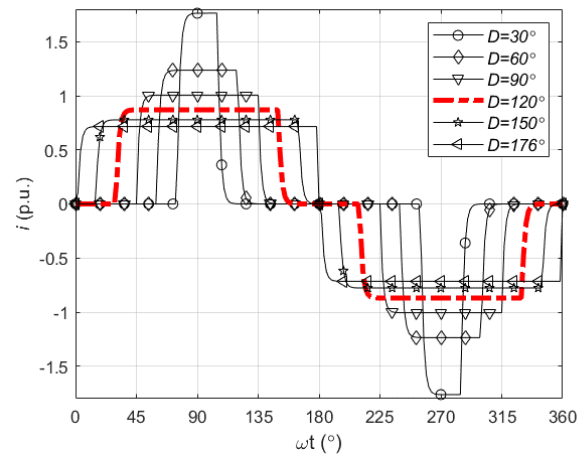


Fig. 5

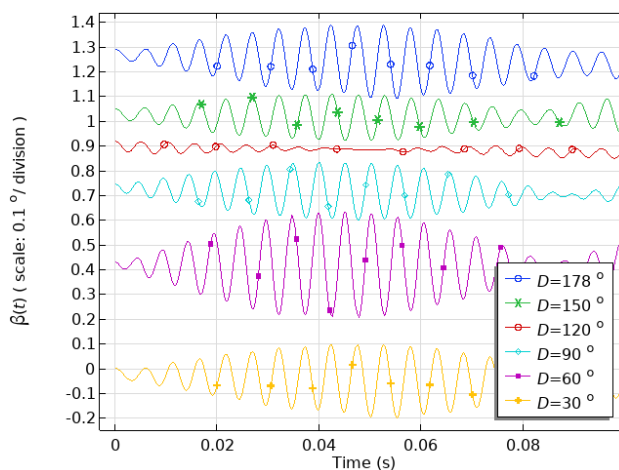


Fig. 6

cores are rotating synchronously. The influence of the windings producing the rotational torque is also neglected. The basic results of the study are as follows.

1. The modeling of nutation swing during the forced precession caused by sinusoidal control current and disturbed sinusoidal one shows that the only precise sinusoidal current waveform gives the minimal nutation swing.
2. The power supply of the control winding by a pulse-wave inverter provides the minimum nutation swing when the angular pulse length is about 120 electrical degrees.
3. Taking into account the geometric data, materials and current density in the control winding, the resulting nutation swing is equal to approximately:
 - 0.05° at sinusoidal control current;
 - 0.025° at ideal constant maximum torque;
 - 0.05° at pulse current with angular pulse length of 120 electric degrees, with the same effective value as for sinusoidal current.

The work was supported by state project "To develop scientific foundations and principles for constructing controlled n -degree-of-freedom magneto-electric systems with extreme characteristics" ("Extremum"), KPKVK 6541030.

1. Wang J., Wang W., Jewel G.W., Howe D. A novel spherical permanent magnet Actuator with Three degrees-of-freedom. *IEEE Transactions on Magnetics*. 1998. Vol. 34. No 4. Pp. 2078-2080.
2. Heya A., Hirata K., Ezaki S., Ota T. Dynamic Analysis of a New Three-Degree-of-Freedom Actuator for Image Stabilization. *IEEE Transactions on Magnetics*. 2017. Vol. 53. Issue 6. Pp. 1563-1567. DOI: <https://doi.org/10.1109/TMAG.2017.2664144>.
3. Heya A., Hirata K. Experimental Verification of Three-Degree-of-Freedom Electromagnetic Actuator for Image Stabilization. *Sensors*. 2020. Vol. 20. Issue 9. 2485. DOI: <https://doi.org/10.3390/s20092485>.
4. Wen Y., Li G., Wang Q., Guo X., Cao W. Modeling and Analysis of Permanent Magnet Spherical Motors by a Multitask Gaussian Process Method and Finite Element Method for Output Torque. *IEEE Transactions on Industrial Electronics*. 2021. Vol. 68. Issue 9. Pp. 8540-8549. DOI: <https://doi.org/10.1109/TIE.2020.3018078>.
5. Wen Y., Li G., Wang Q., Tang R., Liu Y., Li H. Investigation on the Measurement Method for Output Torque of a Spherical Motor. *Appl. Science*. 2020. Vol. 10. Issue 7. 2510. DOI: <https://doi.org/10.3390/app10072510>.
6. Lee H.J., Park H.J., Ryu G.H., Oh S.Y., Lee J. Performance Improvement of Operating Three-Degree-of-Freedom Spherical Permanent-Magnet Motor. *IEEE Transactions on Magnetics*. 2012. Vol. 48. No 11. Pp. 4654-4657. DOI: <https://doi.org/10.1109/TMAG.2012.2200470>.
7. Li Z., Chen Q., Wang Q. Analysis of Multi-Physics Coupling Field of Multi-Degree-of-Freedom Permanent Magnet Spherical Motor. *IEEE Transactions on Magnetics*. 2019. Vol. 55. No 6. Pp. 1-5. Art no 8201505. DOI: <https://doi.org/10.1109/TMAG.2019.2899259>.
8. Wenqiang Tao, Guoli Li, Lufeng Ju, Rui Zhou, Cungang Hu. Design and Analysis of a Novel Spherical Motor Based on the Principle of Reluctance. *IEEE International Power Electronics and Application Conference and Exposition (PEAC)*, Shenzhen, China, 07-04 November 2018. Pp. 7-13. DOI: <https://doi.org/10.1109/PEAC.2018.8590483>.
9. Antonov A.E. Electrical machines of magneto-electrical type. Kyiv: Institute of Electrodynamics National Academy of Sciences of Ukraine, 2011. 216 p. (Rus)
10. Milyakh A.N., Barabanov V.A., Dvoynikh V.V. Three-degrees-of-freedom electric machines. *Trekhstepennyye elektricheskie mashiny*. Kyiv: Naukova dumka, 1979. 308 p. (Rus)
11. Magnus K. *Theorie und Anwendungen*. Berlin: Springer, 1971. 493 p.
12. Petrishchev V.F. *Elements of the gyroscope theory and its application for spacecraft control*. Samara: Samarskii gosudarstvennyi aerokosmicheskii universitet, 2004. 68 p. (Rus)
13. Comsol multiphysics modeling and simulation software. URL: <https://www.comsol.ru/documentation> (accessed date 28.07.2023).
14. Shuster M.D. A survey of attitude representations. *Journal of the Astronautical Sciences*. 1993. Vol. 41. No 4. Pp. 439-517.
15. Petukhov I.S. Electromagnetic moments of controlling the precession movement of a three-degree-of-freedom electric machine *Tekhnichna elektrodynamika*. 2023. No 4. Pp. 52-61. DOI: <https://doi.org/10.15407/techned2023.04.052> (Ukr)

УДК 621.313.84 : 531.383

ВПЛИВ ФОРМИ СТРУМУ УПРАВЛІННЯ НА НУТАЦІЮ ТРИСТУПЕНЕВОЇ ЕЛЕКТРИЧНОЇ МАШИНИ З ЗОВНІШНІМ РОТОРОМ

І.С. Петухов, докт. техн. наук, **К.П. Акинін**, докт. техн. наук, **В.Г. Кіреєв**, канд. техн. наук, **В.А. Лавриненко**
Інститут електродинаміки НАН України,
пр. Берестейський, 56, Київ, 03057, Україна.
E-mail: igor_petu@ukr.net.

Розглянуто конструкцію електричної машини з трьома ступенями свободи ротора із зовнішнім магнітопроводом, що містить постійні магніти, і внутрішнім магнітопроводом. Обидва магнітопроводи є такими, що обертаються. У повітряному проміжку між магнітопроводами розташовано обмотки статора, а саме: обмотка керування та двофазна обмотка обертального руху. Кожна з обмоток живиться змінним струмом відповідної фази. Відзначено позитивну властивість гіростабілізації ротора такої конструкції та негативне явище нутації в умовах вимушеної зміни орієнтації осі обертання. Магнітні втрати в системі відсутні завдяки синхронному обертанню зовнішнього та внутрішнього магнітопроводів. Зроблено припущення про нерухомість центру мас і відсутність будь-яких втрат, які роблять механічну систему неконсервативною. Сформульовано математичну модель механічної системи та модель магнітного поля для розрахунку електромагнітних моментів, що діють на ротор. Отримано вирази для складових електромагнітного моменту для використання в інтерфейсі "Comsol Multiphysics". Вивчено вплив синусоїдального та імпульсного струмів обмотки

управління на розмах нутації. Зроблено висновок про оптимальність живлення обмотки керування неспотвореним синусоїдальним струмом або імпульсним струмом з тривалістю прямокутних імпульсів близько однієї третини періоду. Бібл. 15, рис. 6., табл. 1.

Ключові слова: триступенева електрична машина, гіростабілізація, електромагнітний момент, обмотка управління, прецесія, нутація.

1. Wang J., Wang W., Jewel G.W., Howe D. A novel spherical permanent magnet Actuator with Three degrees-of-freedom. *IEEE Transactions on Magnetics*. 1998. Vol. 34. No 4. Pp. 2078-2080.
2. Heya A., Hirata K., Ezaki S., Ota T. Dynamic Analysis of a New Three-Degree-of-Freedom Actuator for Image Stabilization. *IEEE Transactions on Magnetics*. 2017. Vol. 53. Issue 6. Pp. 1563-1567. DOI: <https://doi.org/10.1109/TMAG.2017.2664144>.
3. Heya A., Hirata K. Experimental Verification of Three-Degree-of-Freedom Electromagnetic Actuator for Image Stabilization. *Sensors*. 2020. Vol. 20. Issue 9. 2485. DOI: <https://doi.org/10.3390/s20092485>.
4. Wen Y., Li G., Wang Q., Guo X., Cao W. Modeling and Analysis of Permanent Magnet Spherical Motors by a Multitask Gaussian Process Method and Finite Element Method for Output Torque. *IEEE Transactions on Industrial Electronics*. 2021. Vol. 68. Issue 9. Pp. 8540-8549. DOI: <https://doi.org/10.1109/TIE.2020.3018078>.
5. Wen Y., Li G., Wang Q., Tang R., Liu Y., Li H. Investigation on the Measurement Method for Output Torque of a Spherical Motor. *Appl. Science*. 2020. Vol. 10. Issue 7. 2510. DOI: <https://doi.org/10.3390/app10072510>.
6. Lee H.J., Park H.J., Ryu G.H., Oh S.Y., Lee J. Performance Improvement of Operating Three-Degree-of-Freedom Spherical Permanent-Magnet Motor. *IEEE Transactions on Magnetics*. 2012. Vol. 48. No 11. Pp. 4654-4657. DOI: <https://doi.org/10.1109/TMAG.2012.2200470>.
7. Li Z., Chen Q., Wang Q. Analysis of Multi-Physics Coupling Field of Multi-Degree-of-Freedom Permanent Magnet Spherical Motor. *IEEE Transactions on Magnetics*. 2019. Vol. 55. No 6. Pp. 1-5. Art no 8201505. DOI: <https://doi.org/10.1109/TMAG.2019.2899259>.
8. Wenqiang Tao, Guoli Li, Lufeng Ju, Rui Zhou, Cungang Hu. Design and Analysis of a Novel Spherical Motor Based on the Principle of Reluctance. *IEEE International Power Electronics and Application Conference and Exposition (PEAC)*, Shenzhen, China, 07-04 November 2018. Pp. 7-13. DOI: <https://doi.org/10.1109/PEAC.2018.8590483>.
9. Антонов А.Е. Электрические машины магнитоэлектрического типа. Киев: Институт электродинамики НАН Украины, 2011. 216 с.
10. Милых А.Н., Барабанов В.А., Двойных В.В. Трехстепенные электрические машины. Киев: Наукова думка, 1979. 308 с.
11. Magnus K. *Theorie und Anwendungen*. Berlin: Springer, 1971. 493 p.
12. Петрищев В.Ф. Элементы теории гироскопа и его применение для управления космическими аппаратами. Самара: Самарский гос. аэрокосм. ун-т., 2004. 68 с.
13. Comsol multiphysics modeling and simulation software. URL: <https://www.comsol.ru/documentation> (дата доступу 28.07.2023).
14. Shuster M.D. A survey of attitude representations. *Journal of the Astronautical Sciences*. 1993. Vol. 41. No 4. Pp. 439-517.
15. Петухов І.С. Електромагнітні моменти управління прецесійним рухом триступеневої електричної машини. *Технічна електродинаміка*. 2023. № 4. С. 52-61. DOI: <https://doi.org/10.15407/techned2023.04.052>.

Надійшла 14.08.2023
Остаточний варіант 09.10.2023